Available online at www.sciencedirect.com
SCIENCE DIRECT®
Polyhedron 23 (2004) 1505–1518
POLYHEDRON
www.elsevier.com/locate/poly

Solid state coordination chemistry of mononuclear mixed-ligand complexes of Ni(II), Cu(II) and Zn(II) with α-hydroxycarboxylic acids and imidazole ☆

R. Carballo [a,*], A. Castiñeiras [b], B. Covelo [a], E. García-Martínez [a], J. Niclós [c], E.M. Vázquez-López [a]

[a] *Departamento de Química Inorgánica, Facultade de Ciencias-Quimica, Universidade de Vigo, E-36200 Vigo, Galicia, Spain*
[b] *Departamento de Química Inorgánica, Facultade de Farmacia, Universidade de Santiago de Compostela, E-15706 Santiago de Compostela, Galicia, Spain*
[c] *Departamento de Química Inorgánica, Facultad de Farmacia, Universidad de Granada, E-18071 Granada, Spain*

Received 19 November 2003; accepted 27 February 2004
Available online 27 April 2004

Abstract

Nine mononuclear metal complexes of monoanionic α-hydroxycarboxylates (HL′) with imidazole as a co-ligand have been synthesised and structurally characterized by X-ray diffraction. The nickel(II) complexes can be described by two formulae: $[Ni(HL')_2(Im)_2]$, HL′ = 2-methyllactate (HmL) (**1**) or mandelate (HM) (**2**), and $[Ni(HB)_2(Im)_3]$, HB = benzylate (**3**). In these compounds the nickel atom is in a distorted octahedral environment. The copper(II) complexes of the general formula $[Cu(HL')_2(Im)]$, HL′ = glycolate (HG) (**4**), lactate (HL) (**5**) or 2-methyllactate (HmL) (**6**) presents a square pyramidal coordination geometry with a distortion evaluated in terms of the τ parameter. The zinc(II) complexes have the general formula $[Zn(HL')_2(Im)_2]\cdot xH_2O$, HL′ = lactate (HL) and $x = 1/2$ (**7**), 2-methyllactate (HmL) and $x = 0$ (**8**) and display a distorted octahedral geometry. However, the reaction with H_2B afforded the imidazole complex $[Zn(Im)_6](HB)_2$, HB = benzylate (**9**), which has two uncoordinated benzylate units. In most of the complexes the α-hydroxycarboxylato ligands behave as bidentate monoanionic systems, apart from in **3**, where one ligand is monodentate. All of the complexes are extended into 2D or 3D frameworks through hydrogen bonding. The complexes were also characterized by elemental analysis, FT-IR and UV/Vis spectroscopy. The nickel and copper compounds were also studied by room temperature magnetic susceptibility and room temperature ESR spectra were obtained for the copper compounds. Finally, the thermal behaviour of all the compounds was investigated.

Keywords: Nickel; Copper; Zinc; Imidazole; α-Hydroxycarboxylato complexes; Thermal behaviour; Crystal structures

1. Introduction

An important group of biogenic ligands is represented by the anions of α-hydroxycarboxylic acids. These anions take part in many fundamental biochemical processes, e.g., in the Krebs cycle (malate, citrate, isocitrate), Cory cycle (lactate), photorespiration (glycolate) and others. Elsewhere, α-hydroxycarboxylates, by virtue of their hydroxy and carboxylate functionalities, may also mimic more complex biogenic ligands, e.g., sugars. The imidazole ring, as a histidine moiety, is also present as a ligand toward transition metal ions in a variety of biologically important molecules including non-heme systems and several metalloproteins. These two ligands can simultaneously coordinate metal ions and provide potential intermolecular interactions that allow the formation of supramolecular arrays. Together with the use of these ligands, a selection of individual metal ions with different coordination properties can be a useful tool to generate networks of different dimensionality.

☆ Supplementary data associated with this article can be found, in the online version, at doi:10.1016/j.poly.2004.02.028.

* Corresponding author. Tel.: 34-986-812273; fax: 34-986812556.
E-mail address: rcrial@uvigo.es (R. Carballo).

0277-5387/$ - see front matter © 2004 Elsevier Ltd. All rights reserved.
doi:10.1016/j.poly.2004.02.028

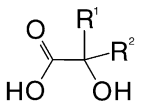

		R^1	R^2
Glycolic acid	H_2G	H	H
Lactic acid	H_2L	H	CH_3
2-Methyllactic acid	H_2mL	CH_3	CH_3
Mandelic acid	H_2M	H	Ph
Benzylic acid	H_2B	Ph	Ph

Scheme 1.

The present paper includes a detailed structural study on the solid state of nickel(II), copper(II) and zinc(II) mixed-ligand complexes with biologically relevant ligands such as α-hydroxycarboxylates and imidazole. For this study, five α-hydroxycarboxylic acids with different levels of bulkiness (Scheme 1) were selected: Glycolic (H_2G), Lactic (H_2L), 2-methyllactic (H_2mL), Mandelic (H_2M) and Benzylic (H_2B) acids.

Previous work in this field has been undertaken by our group and involved the study of mixed-ligand complexes of copper(II) with *N*,*N*-chelating aromatic amines such as 1,10-phenanthroline [1,2] and 2,2′-bipyridine [3,4]. In most of these complexes a pentacoordinated copper(II) ion in a distorted square pyramidal environment is present, but there are also some complexes with an octahedral coordination geometry. The behaviour of the α-hydroxycarboxylic acids in these complexes is very diverse and includes: bidentate monoanion, bidentate dianion, bidentate bridging by the hydroxyl oxygen, monodentate monoanion, monoanionic counterion and also as a neutral molecule in the outer coordination sphere. However, structural studies of first-row transition metal complexes of α-hydroxycarboxylates with monodentate N-donor ligands are not common. To the best of our knowledge the only structural reports in this area concern the glycolate ligand and NH_3 or pyridine as monodentate N-donor ligands: $[Ni(HG)_2(py)_2]\cdot 2H_2O$ [5], $[Cu(HG)_2(NH_3)_2]$ and $[Cu(HG)_2(py)_2]$ [6] contain bidentate monoanionic ligands and the dinuclear copper compound $[Cu_2G_2(py)_2]$ ethane-1,2-diol solvate [7], which contains a bridging bidentate dianionic glycolate ligand.

2. Results and discussion

Reaction of the α-hydroxycarboxylic acids and imidazole in EtOH and/or H_2O with $Ni(AcO)_2\cdot 4H_2O$, $CuCO_3\cdot Cu(OH)_2\cdot 1/2H_2O$ and $ZnCO_3$ led to the isolation of the crystalline products **1**–**9** after slow evaporation of the mother liquors (compounds **2**, **4** and **9**) or after the redissolution of oils or powders obtained in the reactions in MeOH/*i*PrOH (compounds **1**, **3**, **5**, **6** and **8**) or in MeOH/acetone (compound **7**). The yields are high for **1** and **2**, around 50% for **4**–**7** and low for **3**, **8** and **9**. The complexes are air-stable, with melting or decomposition points above 250 °C (**1, 2**), around 200 °C (**4**–**6**) and slightly above 100 °C for the zinc compounds. The complexes are soluble in water, methanol, ethanol and slightly soluble in chlorinated solvents.

2.1. Crystal structures

Metal–ligand bond distances and angles are listed in Table 1. Figs. 1–7 show drawings of the molecular structures together with the atom-numbering schemes used.

The Ni(II) compounds **1** and **2** (Fig. 1 shows compound **2**) and the Zn(II) compounds **7** (Fig. 2) and **8** (Fig. 3) have structures based on neutral complexes $[M(HL')_2(Im)_2]$, where HL′ is a monoanionic *O*,*O*′-bidentate α-hydroxycarboxylato ligand (2-methyllactato for **1** and **8**, lactato for **7** and mandelato for **2**) that chelates the M^{2+} ion through the carboxylato and the hydroxyl oxygen atoms to form a five-membered chelate ring. In this chelate ring the two imidazole ligands are *cis* to each other and *trans* to the hydroxyl oxygen atoms when the metal ion is nickel, but *trans* to the carboxylato oxygen atom in the zinc compound **8**. In compounds **1** and **2** the hydroxyl groups of the two ligands are mutually *cis*, but in **8** they are mutually *trans* in a similar way to the aqua-complex $[Zn(HmL)_2(H_2O)_2]$ [8]. In compound **7** an *all cis* configuration is found. The structure of the nickel compound **3** (Fig. 4) corresponds to neutral molecules $[Ni(HB)_2(Im)_3]$ with a *fac*-disposition of the ligands. In this arrangement one HB ligand acts as a monoanionic *O*,*O*′-bidentate chelating system but the other HB ligand is monoanionic unidentate, so the coordination of the hydroxyl group of one HB ligand is replaced by the coordination of a third imidazole molecule. It therefore appears that the steric requirements of this ligand favour the coordination of a small monodentate ligand like imidazole over the stabilization provided by chelate formation. In all of these complexes, the coordination polyhedra are distorted octahedral with the main deviations from regularity affecting the chelating angles $O_{hydroxyl}$–M–$O_{carboxy}$ [in the range 76.37°–77.95° for the nickel compounds and 74.68°–76.85° for **7** and **8**]. The Ni–N bond lengths are in the range 2.031–2.077 Å, which is only slightly shorter than that found in the pyridine complex $[Ni(HG)_2(py)_2]\cdot 2H_2O$ [5]. The Ni–$O_{hydroxyl}$ distances (Table 1) increase slightly on going from **1** (containing the less bulky hydroxycarboxylato ligand) to **3** (with the more bulky ligand) and are longer than those in the nickel(II) pyridine compound with the glycolato ligand [5]. The Ni–$O_{carboxy}$ distances are in the range 2.027–2.0466 Å

Table 1
Selected bond lengths (Å) and angles (°)

Compound	**1**[*]	**2**	**3**	**4** ($\tau = 0.04$)	**5** ($\tau = 0.03$)	**6** ($\tau = 0.29$)	**7**	**8**[**]	**9**[***]
Bond lengths									
M–O11	2.0466(15)	2.029(3)	2.034(4)	1.962(4)	1.952(4)	1.932(3)	2.098(2)	2.117(2)	
M–O21		2.027(4)	2.155(4)	1.945(4)	1.920(4)	1.956(3)	2.079(2)		
M–N1	2.0632(17)	2.034(4)	2.054(5)	1.958(5)	1.944(5)	1.973(3)	2.115(3)	2.094(3)	2.183(2)
M–N3		2.031(4)	2.058(5)				2.077(3)		2.190(2)
M–N5			2.077(5)						2.203(2)
M–O13	2.1084(15)	2.122(4)	2.135(4)	2.383(5)	2.284(5)	2.256(3)	2.106(2)	2.113(2)	
M–O23		2.109(4)		1.993(5)	1.969(4)	1.951(3)	2.257(2)		
Bond angles									
O11–M–O11^{i}/O21	172.85(8)	169.40(14)	89.84(15)	173.74(19)	171.22(19)	88.99(11)	87.45(9)	92.09(14)	
O11–M–N1	93.79(6)	94.03(17)	90.52(17)	93.45(19)	94.56(18)	94.54(12)	170.74(10)	88.44(10)	
O11–M–N1^{i}/N3	91.19(6)	93.24(17)	88.36(17)				94.95(10)	170.40(10)	
O11–M–O13	76.41(5)	76.31(14)	77.95(15)	76.14(16)	77.09(17)	76.64(10)	76.85(8)	74.68(9)	
O11–M–O13^{i}/O23	98.33(6)	94.26(15)		91.76(18)	91.08(17)	169.96(11)	87.50(9)	91.55(9)	
O11–M–N5			171.23(18)						
N1–M–N1^{i}/N3	91.79(10)	90.92(19)	92.90(19)				92.94(10)	92.63(16)	90.35(9)
N1–M–O13	91.70(7)	90.90(17)	91.34(18)	95.42(19)	96.2(2)	109.81(12)	86.99(10)	97.83(11)	
N1–M–O13^{i}/O23	167.31(6)	171.15(18)		171.2(2)	169.4(2)	95.18(3)	85.47(10)	95.73(10)	
N1–M–N5			94.61(19)						88.76(9)
O13–M–O13^{i}/O23	87.53(9)	88.04(15)		92.66(19)	93.8(2)	102.35(11)	88.92(9)	160.32(14)	
O21–M–N3		93.05(18)	87.79(17)				96.40(10)		
O21–M–N1		94.40(17)	179.23(17)	92.56(19)	92.14(19)	152.45(12)	96.48(10)		
O21–M–O23		77.03(15)		82.06(18)	81.44(18)	81.22(11)	74.81(8)		
O21–M–O13		97.12(14)	88.07(16)	105.03(18)	107.83(18)	97.60(10)	157.93(9)		
N3–M–O23		91.71(18)					170.79(10)		
N3–M–O13		169.49(19)	165.70(17)				100.28(11)		
N3–M–N5			98.46(19)						91.38(9)
N5–M–O13			94.80(17)						
N5–M–O21			84.96(17)						
N1–M–N3^{i}									89.65(9)
N1–M–N5^{i}									91.24(9)
N3–M–N5^{i}									88.62(9)

[*] $i = -x, y, -z + 1/2$.
[**] $I = -y + 1, -x + 1, -z + 1/2$.
[***] $i = -x + 1, -y + 1, -z$.

when the α-hydroxycarboxylato ligand is a bidentate chelate but in **3**, where one HB ligand acts in a monodentate manner, this bond length has a larger value (2.155 Å). In the nickel compounds, however, when the anionic ligand acts as a chelating system, the Ni–$O_{hydroxyl}$ bonds are longer than the Ni–$O_{carboxy}$ bonds. In **7** and **8** the Zn–N bond lengths are shorter than those observed in hexakis-substituted imidazole complexes (compound **9** in this work and [9]) but slightly longer than those found in other bis-substituted systems [10–12]. The Zn–$O_{hydroxyl}$ and Zn–$O_{carboxy}$ distances are longer than the corresponding distances observed in $[Zn(HmL)_2(H_2O)_2]$ [8].

In compounds **4**–**6** the asymmetric unit is composed of the neutral complex $[Cu(HL')_2(Im)]$ where HL′ = HG (**4**), L = HL (**5**) and L = HmL (**6**). In these three compounds the copper atom is pentacoordinated and the α-hydroxycarboxylato ligands acts as monoanionic *O*,*O*′-bidentate chelate systems. The resulting coordination polyhedra are square pyramids, which are almost perfect for **4** and **5** (Fig. 5 shows compound **5**) but with a slight deviation towards a trigonal bipyramid in **6** (Fig. 6) (Addison's τ value [13] is 0.04 in **4**, 0.03 in **5** and 0.29 in **6**). The hydroxyl group (O13) of one of the anionic ligands is located at the apex of the square pyramid and there is a correlation between this apical Cu–O distance (Table 2) and the value of the tetragonality parameter *T* (ratio between the mean of the four shortest and largest distances: 0.82 for **4**, 0.85 for **5** and 0.87 for **6**). In the basal plane of **4** and **5** the carboxylato oxygen atoms are mutually *trans* but in **6**, where the ligand is 2-methyllactato, they are mutually *cis*. The chelate angles $O_{carboxy}$–Cu–$O_{hydroxyl}$ (range 76.14°–77.09°) have similar values to those observed in the nickel complexes. The Cu–N bond lengths agree with those reported for other copper(II) complexes with imidazole [14,15]. Both the apical and the basal Cu–$O_{hydroxyl}$ distances decrease on going from **4** to **6** and as usual in square pyramidal copper complexes, the Cu–apex distance Cu–O13 is longer than the bond lengths in the base. The apical Cu–$O_{hydroxyl}$ distances are similar to the Cu–$O_{hydroxyl}$ distances found in hexacoordinated copper(II) α-hydroxycarboxylato complexes with 4,4′-bipyridine [16] or 2,2′-bipyridine [3]. In **6** the basal

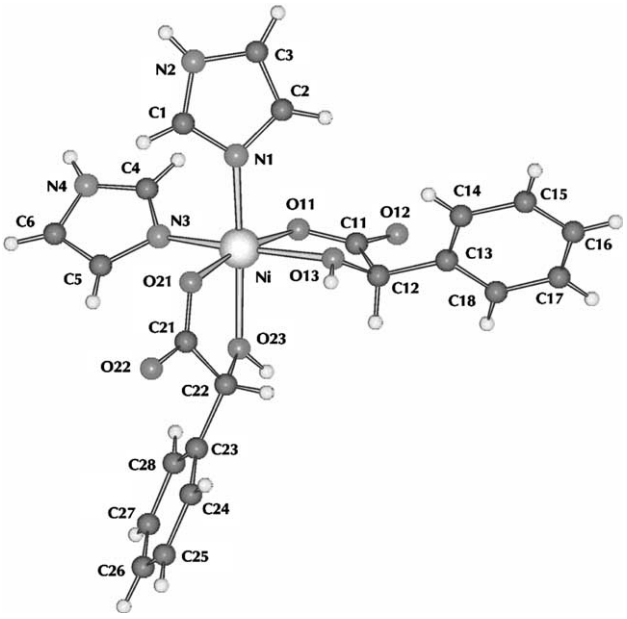

Fig. 1. Molecular structure of $[Ni(HM)_2(Im)_2]$ (**2**), showing the atom numbering scheme.

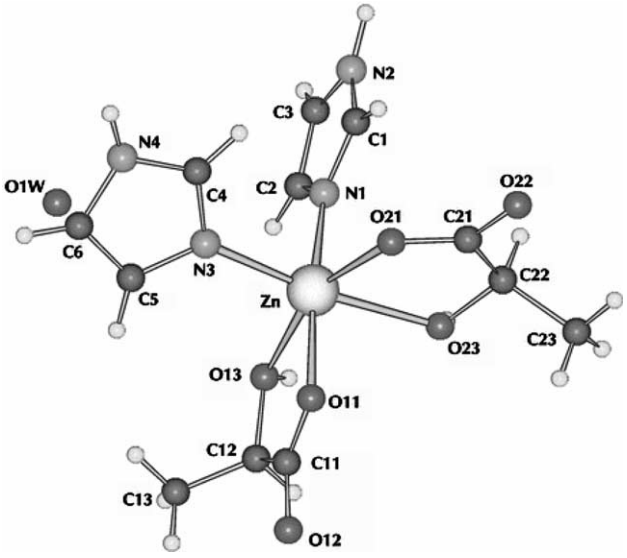

Fig. 2. Molecular structure of *all cis*-$[Zn(HL)_2(Im)_2] \cdot 1/2H_2O$ (**7**).

$Cu–O_{hydroxyl}$ distance is slightly shorter than the $Cu–O_{carboxy}$ distance (belonging the two oxygen atoms of the same ligand). The $Cu–O_{carboxy}$ distances fall within the range usually observed in other copper(II) α-hydroxycarboxylato complexes with N-donor ligands [1–4,16].

The structure of compound **9** is shown in Fig. 7. The zinc ion (located on an inversion centre, d position in the Wyckoff notation) is coordinated to six imidazole ligands and the α-hydroxycarboxylato (benzylato) is present as a monoanionic counterion. Numerous structural reports have been published on octahedral hexakis(imidazole) complexes with first-row transition metals such as Mn(II), Ni(II), Co(II) and Cu(II) but, to the best of our knowledge, only one structure has been reported for a hexakis-substituted complex with Zn(II): $[Zn(Im)_6]Cl_2 \cdot 4H_2O$ [9]. As required by symmetry, the imidazole rings in a *trans* arrangement are coplanar and the metal ion also lies in this plane. The Zn–N distances (Table 1) are similar to those found in $[Zn(Im)_6]Cl_2 \cdot 4H_2O$ [9].

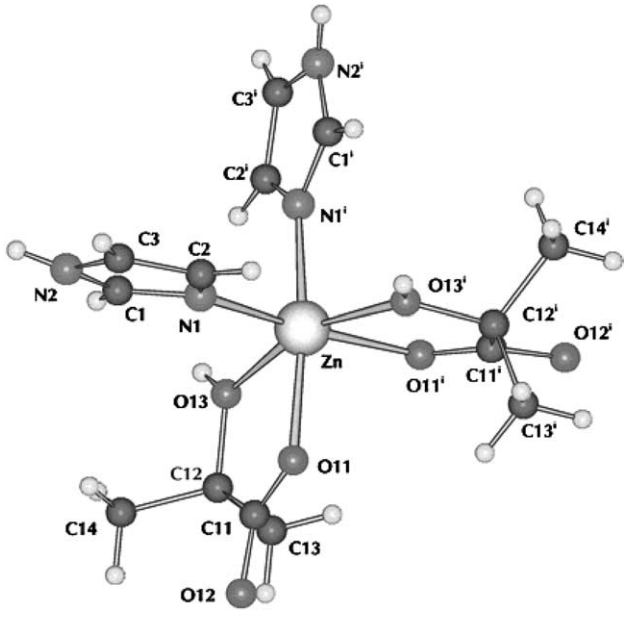

Fig. 3. Molecular structure of $[Zn(HmL)_2(Im)_2]$ (**8**).

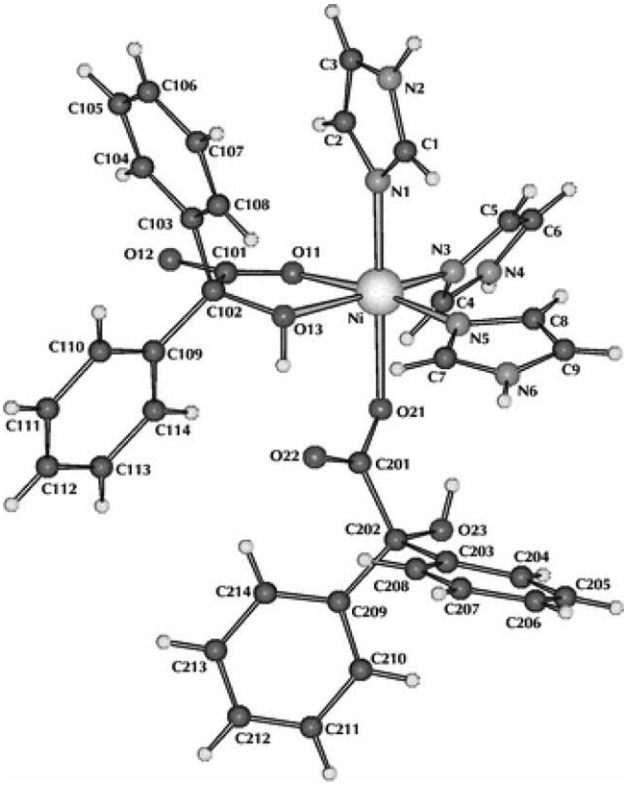

Fig. 4. Molecular structure of *fac*-$[Ni(HB)_2(Im)_3]$ (**3**).

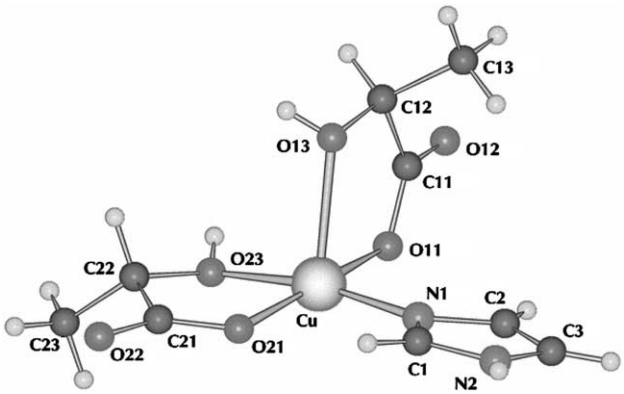

Fig. 5. Molecular structure of $[Cu(HL)_2(Im)]$ (**5**).

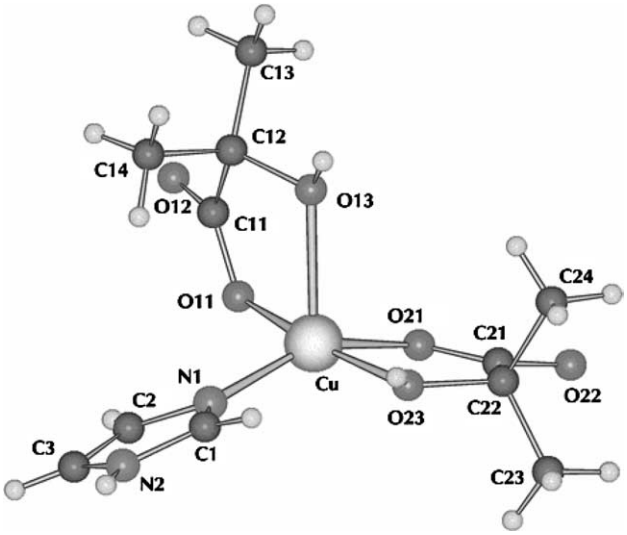

Fig. 6. Molecular structure of $[Cu(HmL)_2(Im)]$ (**6**).

The nature of the imidazole and α-hydroxycarboxylato ligands allows the formation of supramolecular architectures based on hydrogen bonding (Table 2). In most cases, an infinite two-dimensional network is obtained and the 2D structure for **5** is shown in Fig. 8. In complex **3** (Fig. 9), the presence of three imidazole ligands in a *fac*-disposition gives rise to a 3D structure. In all compounds the shortest and most linear intermolecular hydrogen bonds are those between the hydroxyl groups and/or the –NH groups as donors and the uncoordinated oxygen atoms of the carboxylato groups of adjacent molecules as acceptors (O...O range 2.50–2.76 Å and N...O range 2.72–2.95 Å). In addition, other types of intermolecular hydrogen bonds are present in some complexes, where the coordinated $O_{carboxy}$ atom acts as an acceptor and the donors are the –NH groups of the imidazoles (nickel compounds **1** and **3**, N...O distances = 3.004 and 3.191 Å; zinc compound **7**, N...O = distance: 2.799 Å) or the –OH group (copper complexes **5** and **6**, O...O distances = 2.827 and 3.226 Å; zinc compound **7**, O...O distance = 2.785 Å). An interaction between the –NH group and the –OH group acting as an acceptor is also observed in the nickel compound **3** (N...O distance = 2.814 Å) and the zinc compound **9,** where HB acts as a counterion (N...O distance = 3.218 Å). In **4** and **8** there are also C–H...O bonds, which involve imidazole carbons and uncoordinated $O_{carboxy}$ atoms. The values of C...O distances (3.215 and 3.346 Å) and C–H...O angles (152.3° and 161.2°) provide evidence for a significant interaction [17]. This latter bond leads to the formation of 3D networks in **4** (Fig. 10 shows the 2D sheets linked by C–H...O bonds) and in **8** (Fig. 11). In **9** each imidazole ligand participates

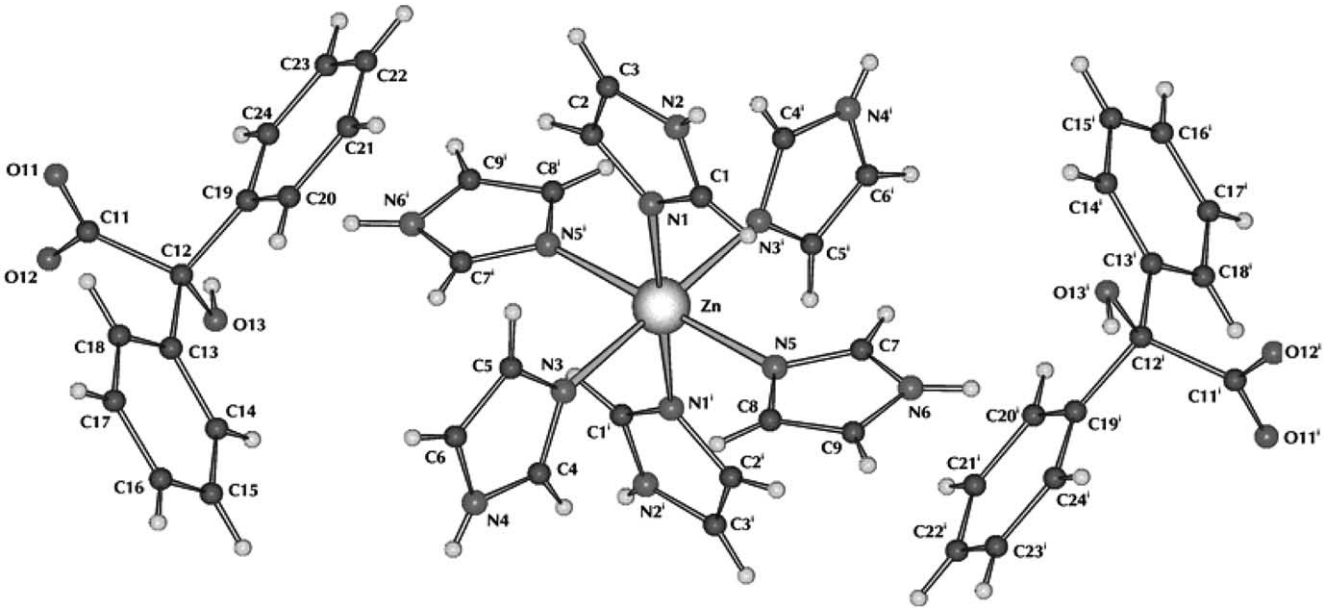

Fig. 7. Molecular structure of $[Zn(Im)_6](HB)_2$ (**9**).

Table 2
Main hydrogen bonds [Å, °]

D–H...A	*d*(D–H)	*d*(H...A)	*d*(D...A)	∠(DHA)
Compound **1** (2D) $i = x, -y+1, z-1/2; ii = x, -y+2, z-1/2$				
N2–H20...O11^{i}	0.874(18)	2.18(2)	3.004(3)	158(3)
N2–H20...O12^{i}	0.874(18)	2.39(3)	3.141(3)	145(3)
O13–H13...O12^{ii}	0.832(17)	1.886(17)	2.716(2)	175(3)
Compound **2** (2D)				
$i = -x, -y, -z+1; ii = -x, -y+1, -z+1; iii = -x+1, -y, -z+1;$				
$iv = -x+1, -y+1, -z+1$				
N2–H20...O22^{iii}	0.86	2.00	2.812(6)	158.2
N4–H40...O12^{iv}	0.86	1.99	2.827(5)	163.3
O13–H13...O22^{i}	0.876(19)	1.77(2)	2.620(5)	162(5)
O23–H23...O12^{ii}	0.906(19)	1.72(2)	2.621(5)	173(5)
Compound **3** (3D)				
$i = -x+1, -y, -z+1; ii = x-1/2, -y+1/2, z+1/2; iii = x-1, y, z$				
N2–H20...O12^{ii}	0.99(8)	1.78(8)	2.763(7)	172(7)
N4–H40...O23^{i}	0.89(6)	1.93(6)	2.814(7)	168(6)
N6–H60...O11^{iii}	0.81(7)	2.48(7)	3.191(7)	146(6)
N6–H60...O12^{iii}	0.81(7)	2.25(7)	2.953(8)	145(6)
Compound **4** (3D)				
$i = -x+1, -y+1, -z; ii = -x+2, -y, -z+1; iii = x-1, y, z;$				
$iv = x+1, y+1, z$				
N2–H20...O22^{i}	0.88(6)	1.91(6)	2.787(7)	174(6)
O13–H13...O12^{iii}	0.81(6)	1.98(7)	2.760(6)	161(6)
O23–H23...O12^{ii}	0.71(6)	1.94(7)	2.648(6)	170(7)
C3–H3...O22^{iv}	0.93	2.36	3.215(7)	152.3
Compound **5** (2D) $i = x-1, y, z; ii = -x+1, -y, -z; iii = -x, -y+1, -z$				
N2–H20...O22^{iii}	0.988(5)	1.783(4)	2.721(7)	157.3(3)
O13–H13...O11^{i}	0.823(19)	2.56(4)	3.226(6)	138(6)
O13–H13...O12^{i}	0.823(19)	1.94(3)	2.727(6)	159(7)
O23–H23...O12^{ii}	0.781(19)	1.90(3)	2.642(6)	160(5)
Compound **6** (2D) $i = x+1/2, -y+3/2, z+1/2; ii = x+1, y, z$				
N2–H20...O22^{ii}	0.96(4)	1.82(4)	2.759(5)	166(4)
O23–H23...O12^{i}	0.94(4)	1.67(4)	2.597(4)	166(3)
O13–H13...O21^{i}	0.93(4)	1.91(4)	2.827(4)	167(3)
Compound 7 (2D)				
$i = -x+3/2, -y+1/2, z+1/2; ii = -x+3/2, y+1/2, z : iii = x, -y, z+1/2$				
N2–H20...O11^{i}	0.96(4)	1.86(4)	2.799(4)	167(4)
O13–H13...O22^{ii}	0.79(4)	1.81(4)	2.587(3)	168(4)
O23–H23...O21^{ii}	0.86(4)	1.94(4)	2.785(3)	165(3)
N4–H40...O12^{iii}	0.85(3)	1.92(3)	2.729(4)	160(3)
Compound **8** (3D)				
$i = -x+1/2, y+1/2, -z+3/4; ii = -y+1/2, x+1/2, z-1/4;$				
$iii = -y, -x+1, -z+1/2$				
N2–H20...O12^{iii}	0.84(5)	1.93(5)	2.737(4)	160(4)
O13–H13...O12^{ii}	0.98(6)	1.65(6)	2.623(3)	173(5)
C2–H2...O12^{i}	0.93	2.45	3.346(5)	161.2
Compound **9** (3D)				
$i = -x, -y, -z; ii = -x, -y+1, -z; iii = -x+1, y+1/2, -z+1/2;$				
$iv = x+1, y+1, z$				
N2–H20...O11^{iii}	0.78(4)	1.99(4)	2.762(4)	171(4)
N4–H40...O13^{ii}	0.76(4)	2.54(4)	3.218(4)	150(4)
N4–H40...O12^{ii}	0.76(4)	2.38(4)	3.041(4)	145(4)
N6–H60...O12^{iv}	0.90(3)	1.90(4)	2.793(3)	172(3)
O13–H13...O12^{i}	0.82	2.11	2.918(3)	170.1
C24–H24...O12^{i}	0.93	2.49	3.329(4)	149.8

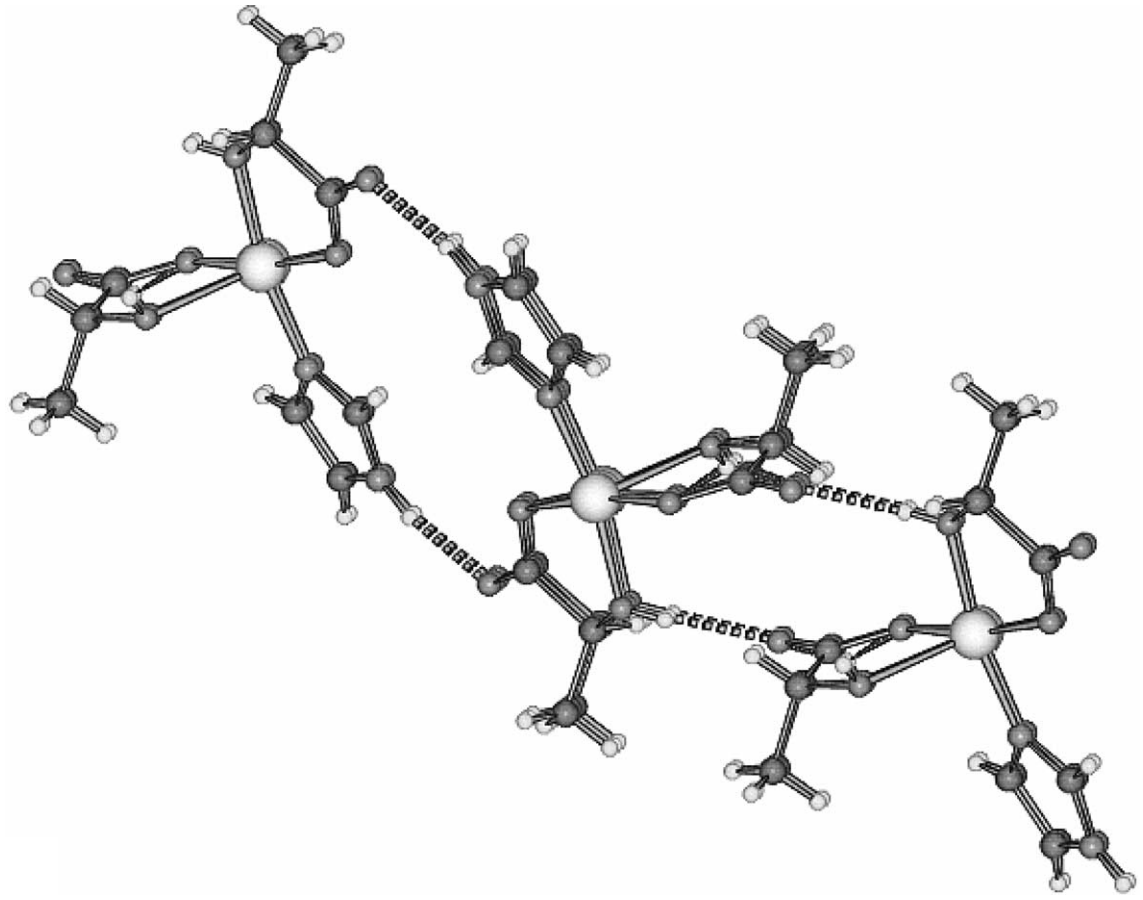

Fig. 8. View of the 2D crystal packing through hydrogen bonding in $[Cu(HL)_2(Im)]$ (**5**).

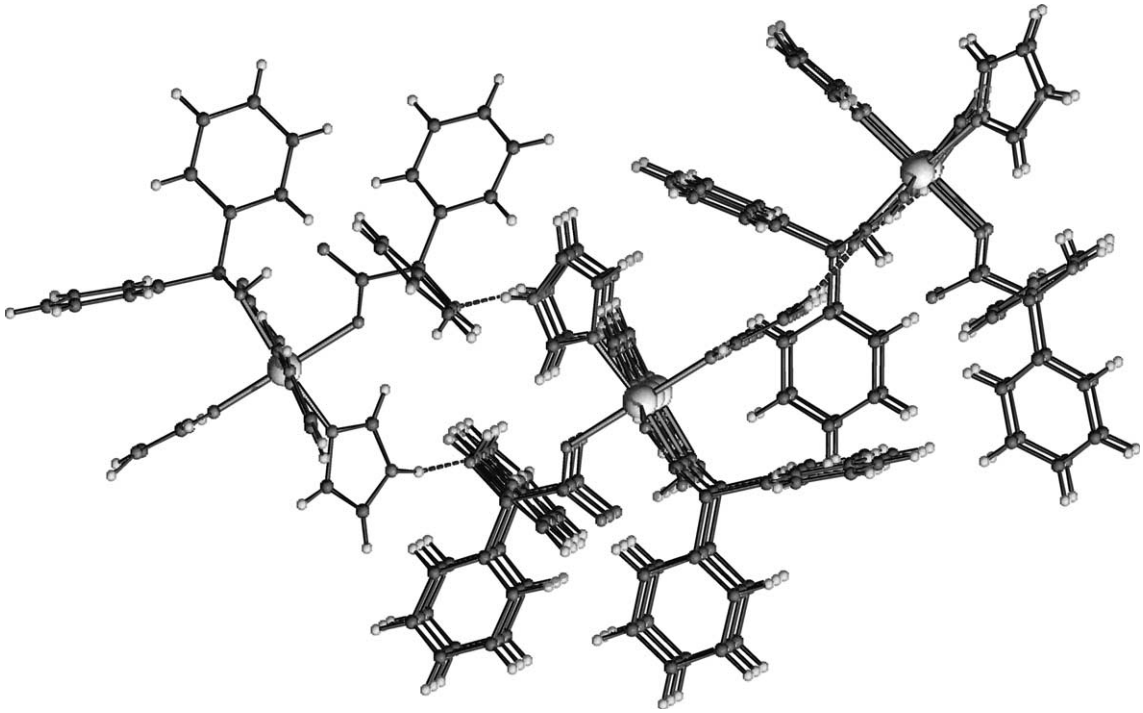

Fig. 9. Crystal packing diagram running along the *a*-axis for $[Ni(HB)_2(Im)_3]$ (**3**).

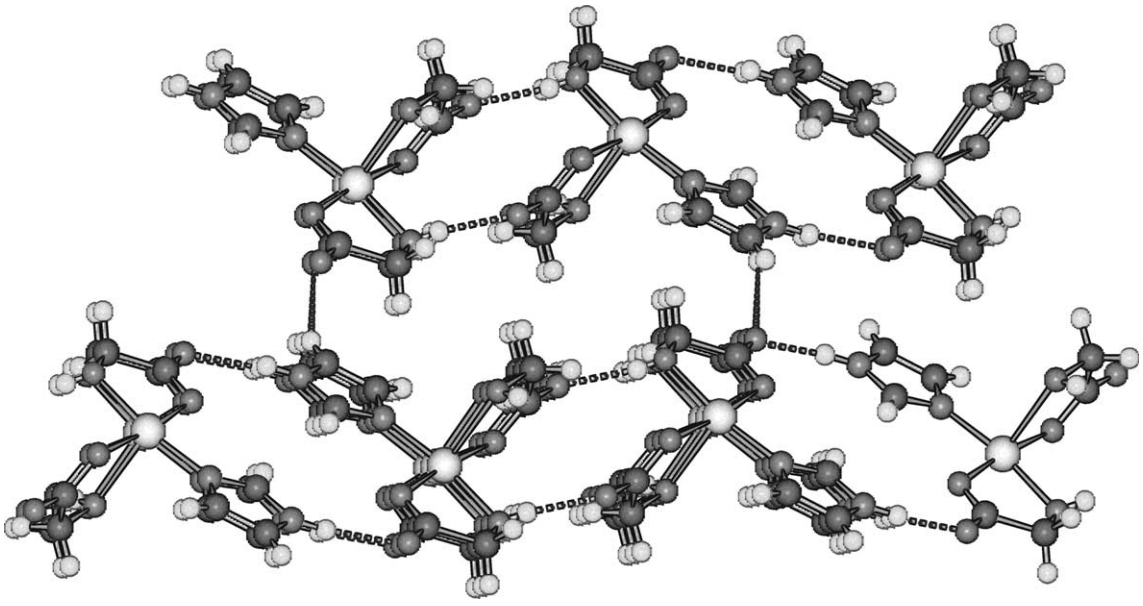

Fig. 10. View of the packing in $[Cu(HG)_2(Im)]$ (**4**) showing the linkage by C–H...O hydrogen bonds of the 2D sheets.

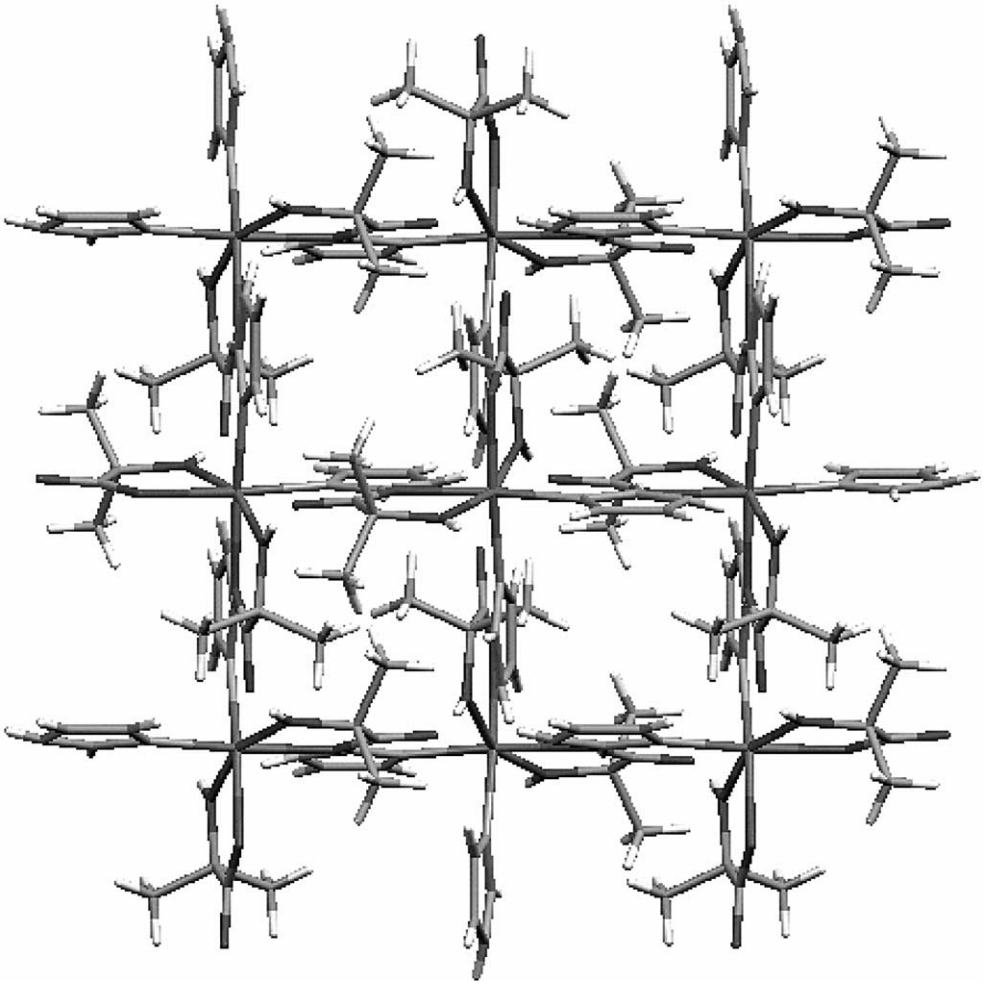

Fig. 11. View of the 3D crystal packing in $[Zn(HmL)_2(Im)_2]$ (**8**) in the ab plane.

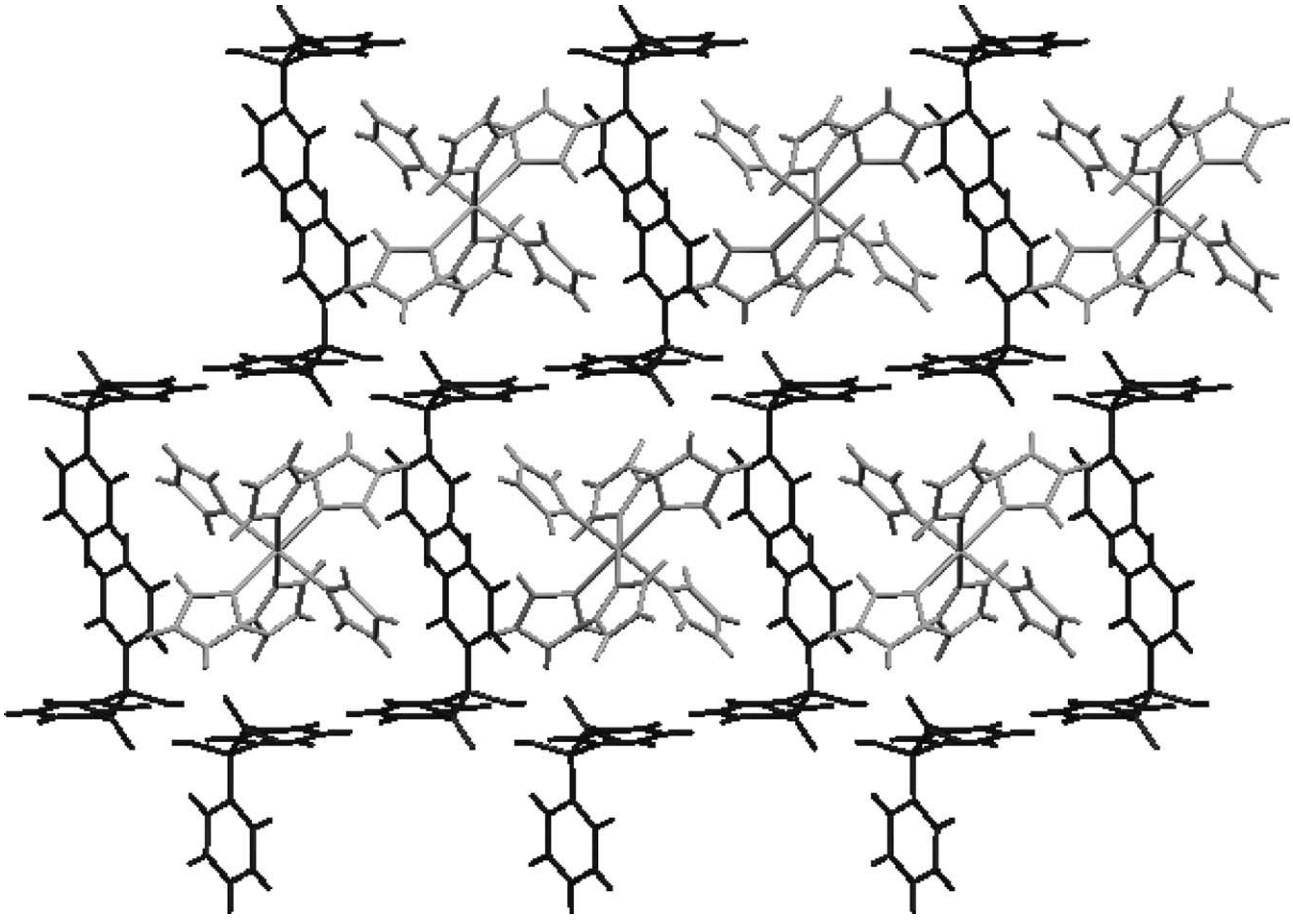

Fig. 12. A fragment of the infinite 3D network through hydrogen bonds of $[Zn(Im)_6](HB)_2$ (**9**) showing the close-packing in the plane *ac*.

in hydrogen bonds with HB molecules, meaning that each cation $[Zn(Im)_6]^{2+}$ is surrounded by six HB molecules and each HB molecule interacts with three cationic species to generate a 3D network (Fig. 12).

All compounds crystallize without solvent molecules in their structures apart from **7**, which contains one water molecule located on a twofold axis (Wyckoff position 4c). This water molecule is not involved in hydrogen bonding.

There are also a number of stacking interactions that involve the imidazole rings. The shortest centroid-to-centroid distances are observed in compounds **4** and **5** (3.581 and 3.571 Å, respectively) with an interplanar dihedral angle α of 0.00° (indicating Im/Im parallelism) and slipping angles β and γ of approximately 24°, revealing a moderate slipping of the stacked rings [18]. Edge-to-face C–H$\ldots\pi$ interactions are also observed in some cases. The main interactions are found in **9** [with an intramolecular C–H(Im)...imidazole centroid of 3.59 Å] and intermolecular interactions in **2** [C–H(Im)... phenyl centroid, 3.52 Å], **4** [C–H(methyl group)... imidazole centroid, 3.49 Å], **5** [C–H(Im)...imidazole centroid, 3.30 Å], **6** [C–H(methyl group)...imidazole centroid,3.67 Å] and **7** [C–H(Im)...imidazole centroid, 3.49 Å].

2.2. Thermal behaviour

Thermogravimetric analysis (TGA) was performed to investigate the thermal stability of compounds **1**–**9**. A summary of the results is given in Table 3. The species were investigated by monitoring the evolved gases by IR spectroscopy. The thermal behaviour of most of the compounds is very similar and generally shows two steps, with the exception of **2** and **9** (three steps) and **7**, which contains water of crystallization (four steps). The nickel and copper compounds are stable up to 170–200 °C and the zinc compounds to 120–150 °C. In **7** the first step corresponds to the loss of the non-coordinated water (75–150 °C). In most of the compounds, however, the first mass loss corresponds to pyrolysis of the α-hydroxycarboxylato ligands followed, in a second step, by the loss of imidazole. Finally, the complexes give residues of NiO at 375–500 °C (nickel compounds), CuO at 425–450 °C (copper compounds) and ZnO or $Zn(OH)_2$ at 475–550 °C (zinc compounds).

Table 3
Summary of thermal, spectral and magnetic properties ($^*\Delta v = v_{as}(OCO) - v_s(OCO)$)

Compound	1	2	3	4	5	6	7	8	9
TG analysis									
Number of steps	2	3	2	2	2	2	4	2	3
T (°C)	200–500	215–400	175–375	200–450	170–450	200–425	75–475	150–550	120–500
1st step loss	HmL	HM	Im	HG	HL	HmL	H_2O	HmL	HB
Other steps loss	Im	Im	HB	Im	Im	Im	HmL, Im	Im	Im
Final residue	NiO	NiO	NiO	CuO	CuO	CuO	ZnO	$Zn(OH)_2$	ZnO
IR data (cm^{-1})									
ν(OH)/ν(NH)	3140 overlap	3240/3139	3400/3178	3230/3137	3399/3169	3279/3142	3388, 3149	3400-3100 overlap	3391, 3216/3133
ν_{as}(OCO)/Im I band	1579/1640	1597 overlap	1599/1620	1597 overlap	1610 overlap	1571/1643	1597 overlap	1589 overlap	1598 overlap
ν_s(OCO)	1401	1379	1362	1377	1380	1379	1388	1362	1367
$\Delta\nu^*$	178	~218	237	~220	~230	192	~209	~227	~231
Electronic spectrum (cm^{-1})	9090 (ν_1), 15 480 (ν_2), 26 740 (ν_3)	9415 (ν_1), 15 200 (ν_2), 25 900 (ν_3)	9900 (ν_1), 15 825 (ν_2), 26 740 (ν_3)	13 850	13 440	12 315			
μ (BM) *at 293 K*	3.21	3.36	2.96	1.86	1.75	2.25			
ESR type				axial	axial	quasi-iso			
$g_{\|}$, $g_{\perp}$				2.31, 2.06	2.31, 2.05				
$g_{average}$						2.13			

2.3. Infrared spectra

The IR spectra of most of the complexes (Table 3) show sharp bands in the 3100–3200 cm^{-1} region, which are assigned to the NH stretching frequency. Complexes **1** and **8** show broad bands in the 3100–3200 cm^{-1} region including ν(OH) and ν(NH) and the remaining complexes show broad bands in the 3200–3400 cm^{-1} region, which correspond to ν(OH). The intense bands appearing around 1600 cm^{-1}, which in most cases overlap with bands associated with the imidazole I band, are assigned to the asymmetric COO^- vibration. The bands found between 1360 and 1400 cm^{-1} are assigned to ν_s(COO). The estimated values around 200 cm^{-1} for $\Delta\nu = \nu_{as}(OCO) - \nu_s(OCO)$ are typical of monodentate carboxylato groups [19]. In compounds **1**–**8** a band is observed in the 420–450 cm^{-1} region and this is attributed to ν(MO) [20].

2.4. Electronic spectra

The reflectance spectra of the nickel and copper complexes in the solid state were recorded in the range 250–1500 nm. The spectra of compounds **1**–**3** (Table 3) are typical of Ni(II) [ground state $^3A_{2g}(F)$] octahedral complexes. The band found between 9090 and 9900 cm^{-1} can be assigned to the $^3T_{2g}(F) \leftarrow {}^3A_{2g}(F)$ (ν_1) transition, that observed around 15 000 cm^{-1} to the $^3T_{1g}(F) \leftarrow {}^3A_{2g}(F)$ (ν_2) transition and the band close to 26 000 cm^{-1} to the $^3T_{1g}(P) \leftarrow {}^3A_{2g}(F)$ (ν_3) transition. The spectra of the copper(II) complexes **4**–**6** all exhibits a broad band, centred at around 13 500 cm^{-1} for **4** and **5** and at 12 300 cm^{-1} for **6**. These bands are characteristic of a copper(II) d–d transition [21] in a tetragonal field in which the copper(II) atom is in a distorted square-based pyramidal coordination environment.

2.5. Magnetic properties

For the nickel complexes (**1**–**3**) the magnitude of the effective magnetic moments between 2.96 and 3.36 BM at room temperature are as one would expect for octahedral symmetry but larger than the spin-only value (2.83 BM) expected for the two unpaired electrons of the Ni(II) cation with a d^8 configuration [22]. For the copper complexes (**4**–**6**), μ_{eff} at room temperature varies from 1.75 to 2.25 BM and these values lie in the range expected for pentacoordinated complexes of copper(II) [23] and are also larger than the spin-only value for an uncoupled Cu(II) ion (1.73 BM).The ESR spectra at room temperature are of the axial type for compounds **4** and **5** ($g_{\|} = 2.31 > g_{|} = 2.06$–$2.05$) and quasi-isotropic or near isotropic ($g_{av} \sim 2.13$) for **6**. These spectra are in accordance with a $d_{x^2-y^2}$ ground state for copper(II), as one would expect for an elongated square-based pyramidal coordination polyhedron.

3. Experimental

3.1. Materials and physical measurements

All reagents and solvents were obtained commercially and were used as supplied.

Microanalyses (C, H, N) were carried out with a FISONS EA-1108 elemental analyser. Melting points (m.p.) were measured with a Gallenkamp MBF-595 apparatus. FT-IR spectra in the 4000–400 cm^{-1}region were recorded from KBr pellets on a Bruker VECTOR 22 spectrophotometer. A Shimadzu UV-3101PC spectrophotometer was used to obtain the electronic spectra in the region 250–1500 nm. ESR spectra of polycrystalline samples were recorded without magnetic dilution using a Bruker ESP 300E spectrophotometer (X band) at room temperature. Magnetic susceptibility measurements were performed at 25 °C using a Johnson Matthey Alfa MSB-MKI Gouy balance. TG/DTG analysis profiles (pyrolysis, 300–1000 K, with IR and MS investigation of evolved gases) were recorded under a 100 mL min^{-1} air flow using a Shimadzu TGA-DTG-50H Thermobalance coupled to a Nicolet Magma 550 FT-IR apparatus and a Fisons Thermolab mass spectrometer.

3.2. Synthesis and crystallisation of the complexes

3.2.1. Nickel(II) Compounds

Compounds **1** and **2** were synthesised by reacting $Ni(AcO)_2 \cdot 4H_2O$ (1 mmol) with 2-methyllactic acid (H_2mL) and mandelic acid (H_2M) (2 mmol), respectively, and Im (2 mmol) in EtOH (30 mL). The mixture was refluxed for 2 h and was then left to cool to room temperature, after which stirring was maintained for 7 days. The light blue powders of **1** and **2** were filtered off. When the reactions were carried out in the molar ratio 1:2:1, the resulting products were respectively: $[Ni(HmL)_2(OH_2)_2]$ (~50%) and **1** (~50%); $[Ni(HM)_2(OH_2)_2]$. H_2O (~50%) and **2** (~50%).

Data for *[Ni(HmL)$_2$(OH$_2$)$_2$]*: m.p.>250 °C. *Anal.* Calc. for $C_8H_{18}O_8Ni$ (300.92): C, 31.9; H, 6.5. Found: C, 32.0; H, 6.2%. IR (ν cm^{-1}): 3448 s, 3193 s, 1624 s, 1487 s, 1174 s. UV–Vis (ν, cm^{-1}): 25 250, 13 625, 8700.

Data for *[Ni(HM)$_2$(OH$_2$)$_2$]·H$_2$O*: m.p.>250 °C. *Anal.* Calc. for $C_{16}H_{20}O_9Ni$ (415.02): C, 46.3; H, 4.9. Found: C, 45.7; H, 4.8%. IR (ν cm^{-1}): 3391 s, 3100 s, 1610 s, 1395 m, 1028 m. UV–Vis (ν, cm^{-1}): 25 640, 13 660, 8350.

*3.2.1.1. [Ni(HmL)$_2$(Im)$_2$] (**1**).* Yield: 81%; m.p. >250 °C. *Anal.* Calc. for $C_{14}H_{22}N_4O_6Ni$ (401.07): C, 41.9; H, 5.1; N, 13.1. Found: C, 41.1; H, 6.1; N, 12.4%. IR (ν cm^{-1}): 3140 vs b, 2975 vs, 1640 vs, 1579 vs, 1491 s, 1401 s, 1175 s, 1073 s, 966 m, 925 s, 824 m, 730 s, 623 m, 432 m.

Recrystallisation from MeOH/*i*PrOH (1:1) of the light blue oil resulting from the slow evaporation of the mother liquor yielded single crystals of **1**.

*3.2.1.2. [Ni(HM)$_2$(Im)$_2$] (**2**).* Yield: 73%; m.p.> 250 °C. *Anal.* Calc. for $C_{22}H_{22}N_4O_6Ni$ (497.15): C, 53.2; H, 4.5; N, 11.3. Found: C, 53.0; H, 4.0; N, 11.0%. IR (ν cm^{-1}): 3240 s, 3139 s, 2956 s, 1597 vs, 1419 s, 1379 s, 1066 s, 944 m, 802 s, 741 s, 698 s, 576 s, 444 m.

Single crystals of **2** were obtained by slow evaporation at room temperature of the filtrate.

*3.2.1.3. [Ni(HB)$_2$(Im)$_3$] (**3**).* Compound **3** was obtained by a similar procedure, but in this case only when the molar ratio 1:2:1 was used was it possible to identify the resulting products. Firstly, a green powder of formula $[Ni(HB)_2(OH_2)_2]$ was isolated from the resulting suspension. Secondly, recrystallisation from MeOH/*i*PrOH (1:1) of the green oil obtained after the slow evaporation of the mother liquor allowed the isolation of single crystals of **3**.

Data for *[Ni(HB)$_2$(OH$_2$)$_2$]*: m.p.>250 °C. *Anal.* Calc. for $C_{28}H_{24}O_8Ni$ (547.18): C, 61.2; H, 4.8. Found: C, 62.1; H, 5.1%. IR (ν cm^{-1}): 3421 s, 1652 s, 1375 m, 1051 m. UV–Vis (ν, cm^{-1}): 23 480, 13 120, 8010.

*[Ni(HB)$_2$(Im)$_3$] (**3**).* Yield: 25%; m.p. 243 °C. *Anal.* Calc. for $C_{37}H_{34}N_6O_6Ni$ (717.41): C, 61.9; H, 4.8; N, 11.7. Found: C, 61.5; H, 4.8; N, 11.5%. IR (ν cm^{-1}): 3400 m b, 3178 s b, 2967 m, 1620 vs, 1599 vs, 1362 s, 1173 m, 1069 s, 942 m, 831 m, 747 s, 699 s, 598 m, 424 w.

3.2.2. Copper(II) compounds

A mixture of $CuCO_3 \cdot Cu(OH)_2 \cdot 1/2H_2O$ (0.5 mmol) and glycolic acid (H_2G) (**4**), lactic acid (H_2L) (**5**) or 2-methyllactic acid (H_2mL) (**6**) (2 mmol) and Im (1 mmol) in H_2O (30 mL) for **4** and in EtOH (30 mL) for **5** and **6** was refluxed for 2 h and then left to cool to room temperature, after which stirring was maintained for several days. The resulting blue solids **4**–**6** were filtered off and dried over $CaCl_2$.

When a molar metal:imidazole ratio of 1:2 was used the same compounds were obtained.

*3.2.2.1. [Cu(HG)$_2$(Im)] (**4**).* Yield: 50%; m.p. 219 °C. Anal. Found: C, 29.7; H, 3.9; N, 9.7. Calcd. for $C_7H_{10}N_2O_6Cu$ (281.71): C, 29.8; H, 3.6; 9.9%. IR (ν cm^{-1}): 3230 m, 3137 m, 2942 m, 1597 vs, 1377 m, 1075 m, 931 w, 841 w, 771 w, 698 w, 550 w, 451 vw.

Single crystals of **4** were obtained by slow concentration of the mother liquor at room temperature.

*3.2.2.2. [Cu(HL)$_2$(Im)] (**5**).* Yield: 56%; m.p. 190 °C. *Anal.* Calc. for $C_9H_{14}N_2O_6Cu$ (309.76): C, 34.9; H, 4.6; N, 9.0. Found: C, 35.1; H, 5.1; N, 9.6%. IR (ν cm^{-1}): 3399 m, 3169 m, 2980 m, 1610 vs, 1380 s, 1102 m, 1077 m, 959 w, 865 m, 769 m, 654 m, 556 m, 425 w.

Table 4
Crystal data and structure refinement

Compound	1	2	3	4	5	6	7	8	9
Empirical formula	$C_{14}H_{22}N_4O_6Ni$	$C_{22}H_{22}N_4O_6Ni$	$C_{37}H_{34}N_6O_6Ni$	$C_7H_{10}N_2O_6Cu$	$C_9H_{14}N_2O_6Cu$	$C_{11}H_{18}N_2O_6Cu$	$C_{12}H_{19}N_4O_{6.5}Zn$	$C_{14}H_{22}N_4O_6Zn$	$C_{46}H_{46}N_{12}O_6Zn$
Formula weight	401.07	497.15	717.41	281.71	309.76	337.81	388.68	407.73	928.32
Crystal system	monoclinic	triclinic	monoclinic	triclinic	monoclinic	monoclinic	orthorhombic	tetragonal	monoclinic
Space group	$C2/c$	$P\bar{1}$	$P2_1/n$	$P\bar{1}$	$P2_1/c$	$P2_1/n$	$Pbcn$	$P4_32_12$	$P2_1/c$
Unit cell dimensions									
a (Å)	19.392(7)	9.170(3)	9.2191(11)	5.528(2)	5.422(3)	9.6623(15)	20.4557(18)	10.7634(9)	12.9507(17)
b (Å)	8.477(3)	10.936(3)	29.972(4)	7.267(3)	13.436(7)	17.630(3)	10.4408(9)	10. 7634(9)	9.0191(11)
c (Å)	11.412(4)	12.717(4)	12.5644(15)	13.626(5)	17.000(9)	9.7978(16)	15. 0918(13)	16.442(3)	22.209(3)
α (°)		106.910(7)		75.045(5)					
β (°)	111.795(7)	110.208(6)	94.428(3)	85.826(6)	92.324(11)	118.748(3)			119.763(6)
γ (°)		90.172(7)		75.613(7)					
Volume (Å^3)	1741.9(11)	1137.4(6)	3461.3(7)	512.2(3)	1237.4(11)	1463.3(4)	3223.2(5)	1904.8(4)	2251.9(5)
Z, ρ_{calc} (g cm^{-3})	4, 1.529	2, 1.452	4, 1.377	2, 1.826	4, 1.663	4, 1.533	8, 1.602	4, 1.422	2, 1.369
$F(000)$	840	516	1496	286	636	700	1608	848	968
Crystal size (mm^3)	$0.25 \times 0.21 \times 0.19$	$0.23 \times 0.07 \times 0.06$	$0.25 \times 0.17 \times 0.16$	$0.15 \times 0.13 \times 0.09$	$0.15 \times 0.08 \times 0.\ 08$	$0.18 \times 0.08 \times 0.08$	$0.35 \times 0.30 \times 0.20$	$0.45 \times 0.38 \times 0.32$	$0.30 \times 0.26 \times 0.23$
Absorption coefficient (mm^{-1})	1.152	0.899	0.616	2.148	1.786	1.518	1.564	1.325	0.608
θ Range (°)	2.26–26.37	1.80–28.03	1.36–28.07	1.55–28.07	1.93–27.98	2.43–28.00	1.99–28.05	2.26–23.25	1.81–28.03
Maximum/minimum transmission	1.0000/0.8297	1.0000/0.7469	1.0000/0.8782	1.0000/0.6652	1.0000/0.7576	1.0000/0.8787	1.0000/0.7300	1.0000/0.9429	1.0000/0.9374
Reflections collected	4760	6291	18394	2335	6303	8121	17452	8295	12 535
Independent reflections (R_{int})	1763 (0.0308)	4405 (0.0628)	7653(0.0885)	1984 (0.0229)	2705 (0.0864)	3293(0.0736)	3852(0.0610)	1366(0.0231)	5094(0.0446)
Final R indices	$R_1 = 0.0317$	$R_1 = 0.0541$	$R_1 = 0.1058$	$R_1 = 0.0675$	$R_1 = 0.0495$	$R_1 = 0.0448$	$R_1 = 0.0401$	$R_1 = 0.0326$	$R_1 = 0.0620$
$[I > 2\sigma(I)]$	$wR_2 = 0.0664$	$wR_2 = 0.0629$	$wR_2 = 0.1619$	$wR_2 = 0.1157$	$wR_2 = 0.0686$	$wR_2 = 0.0511$	$wR_2 = 0.0869$	$wR_2 = 0.0809$	$wR_2 = 0.1013$

The recrystallisation of **5** from a 1:1 mixture of MeOH/*i*PrOH yielded blue single crystals.

*3.2.2.3. [Cu(HmL)$_2$(Im)] (**6**).* Yield: 46%; m.p. 200 °C. *Anal.* Calc. for $C_{11}H_{18}N_2O_6Cu$ (337.81): C, 39.1; H, 5.4; N, 8.3. Found: C, 39.1; H, 5.8; N, 8.3%. IR (ν cm^{-1}): 3279 m b, 3142 s, 2978 s, 1643 vs, 1571 s, 1548 s, 1379 s, 1349 s, 1174 s, 1076 m, 960 m, 817 s, 777 m, 622 m, 527 w, 434 w.

Recrystallisation from MeOH/*i*PrOH (1:1) of the blue oil resulting from the slow evaporation of the mother liquor yielded single crystals.

3.2.3. Zinc(II) compounds

A solution of lactic acid (H_2L) (**7**), 2-methyllactic acid (H_2mL) (**8**) or benzylic acid (H_2B) (**9**) (2 mmol) in ethanol (10 mL) and a solution of Im (2 mmol) in EtOH (10 mL) were added to a suspension of $ZnCO_3$ (1 mmol) in EtOH (10 mL). The mixture was refluxed for 2 h and the resulting white suspension was stirred for several days. The resulting white solids were filtered off and dried. Identification of the solid proved impossible in the reaction with 2-methyllactic acid, but with benzylic acid the solid corresponds to a compound of the formula $[Zn(HB)_2(OH_2)_2]$ and that obtained with lactic acid is consistent with the formula $[Zn(HL)_2(Im)_2]\cdot 1/2H_2O$.

Slow evaporation of the mother liquors of **7** and **8** gave colourless oils, which were dissolved in MeOH/acetone (1:1) for **7** and MeOH/*i*PrOH (1:1) for **8**. Slow solvent evaporation led to the isolation of single crystals of **7** and **8**.

*3.2.3.1. [Zn(HL)$_2$(Im)$_2$]·1/2H$_2$O (**7**).* Yield: 42%; m.p. 104 °C. *Anal.* Calc. for $C_{12}H_{19}N_4O_{6.5}Zn$ (388.68): C, 37.1; H, 4.9; N, 14.4. Found: C, 36.3; H, 4.8; N, 14.1%. IR (ν cm^{-1}): 3388 s b, 3149 s, 2934 m, 1597 vs, 1456 m, 1388 s, 1118 s, 1074 s, 948 m, 831 m, 769 m, 661 s, 557 m, 444 m. ^{1}H NMR (400 MHz, D_2O, ppm): imidazole, 8.15 (s, 1H), 7.32 (s, 2H); lactate, 4.20 (q, 1H), 1.38 (d, 3H).

*3.2.3.2. [Zn(HmL)$_2$(Im)$_2$] (**8**).* Yield: 15%; m.p. 164 °C. *Anal.* Calc. for $C_{14}H_{22}N_4O_6Zn$ (407.73): C, 41.2; H, 5.4; N, 13.7. Found: C, 41.2; H, 5.4; N, 14.1%. IR (ν cm^{-1}): 3400 sh, 3118 vs, 2971 vs, 1589 vs b, 1489 vs, 1362 vs, 1176 vs, 1074 vs, 943 s, 861 s, 731 s, 663 s, 562 m, 432 m. ^{1}H NMR (400 MHz, D_2O, ppm): imidazole, 8.10 (s, 1H), 7.29 (s, 2H); 2-methyllactate, 1.42 (s, 6H).

*3.2.3.3. [Zn(Im)$_6$](HB)$_2$ (**9**).* Yield: 35%; m.p. 130 °C. *Anal.* Calc. for $C_{46}H_{46}N_{12}O_6Zn$ (928.32): C, 59.5; H, 5.0; N, 18.1. Found: C, 59.4; H, 5.0; N, 18.2%. IR (ν cm^{-1}): 3391 s, 3216 s, 3133 s, 2933 s, 1598 vs, 1367 vs, 1146 m, 1098 m, 936 s, 831 s, 773 s, 616 s, 582 m. ^{1}H NMR (400 MHz, D_2O, ppm): imidazole, 7.98 (s, 3H), 7.25 (s, 6H); benzylate, 7.45 (s, 10H).

Slow evaporation of the mother liquor from the reaction with benzylic acid afforded colourless single crystals of **9**.

3.3. X-ray structure determination

Crystallographic data were collected on a Bruker Smart CCD diffractometer at 293 K using graphite-monochromated Mo Kα radiation ($\lambda = 0.71073$ Å). The data were corrected for absorption using the program SADABS [24]. The structures were solved by direct methods using the program SHELXS-97 [25]. All non-hydrogen atoms were refined with anisotropic thermal parameters by full-matrix least-squares calculations on F^2 using the program SHELXL-97 [26]. Hydrogen atoms were inserted at calculated positions and constrained with isotropic thermal parameters, except for those of the hydroxyl groups and of the nitrogen atom in imidazole, which were generally located using a Fourier difference map and refined isotropically. For **8**, which crystallized in the chiral space group $P4_32_12$, the absolute structure parameter of 0.47(3) indicated a twinning by inversion [27] of the crystals. Disorder was observed in some carbon atoms of the phenyl groups in **3** and, consequently, the agreement factors R_1 and wR_2 have unusually high values. Drawings were produced with SCHAKAL [28]. Special computations for the crystal structure discussions were carried out with PLATON for Linux [29]. Crystal data and structure refinement parameters are listed in Table 4.

4. Supplementary material

Crystallographic data for the structural analysis have been deposited with the Cambridge Crystallographic Data Centre, CCDC Nos. 224575–224583. Copies of this information may be obtained free of charge from The Director, CCDC, 12 Union Road, Cambridge, CB2 1EZ, UK (fax: +44-1223-336033; e-mail: deposit@ccdc.cam.ac.uk or www: http://www.ccdc.cam.ac.uk).

Acknowledgements

Financial support from ERDF (EU) and DGI-MCYT (Spain) (research projects BQU2002-03543 and BQU2002-04523) is gratefully acknowledged.

References

[1] R. Carballo, B. Covelo, S. Balboa, A. Castiñeiras, J. Niclós, Z. Anorg. Allg. Chem. 627 (2001) 948.
[2] R. Carballo, B. Covelo, E.M. Vázquez-López, A. Castiñeiras, J. Niclós, Z. Naturforsch. 58b (2003) 151.
[3] R. Carballo, A. Castiñeiras, S. Balboa, B. Covelo, J. Niclós, Polyhedron 21 (2002) 2811.

[4] A. Castiñeiras, S. Balboa, E. Bermejo, R. Carballo, B. Covelo, J. Borrás, J.A. Real, Z. Anorg. Allg. Chem. 628 (2002) 1116.
[5] G. Medina, S. Bernès, A. Martínez, L. Gasque, J. Coord. Chem. 54 (2001) 267.
[6] K. Prout, V.S.B. Mtetwa, F.J.C. Rossotti, Acta Crystallogr. B49 (1993) 73.
[7] M. Lanfranchi, L. Prati, M. Rossi, A. Tiripicchio, J. Chem. Soc., Chem. Commun. (1993) 1698.
[8] R. Carballo, B. Covelo, E. García-Martínez, E.M. Vázquez-López, A. Castiñeiras, J. Niclós, Polyhedron 22 (2003) 1051.
[9] T.P.J. Garret, J.M. Guss, H.C. Freeman, Acta Crystallogr. C39 (1983) 1027.
[10] C.-D. Wu, C.-Z. Lu, D.-M. Wu, H.-H. Zhuang, J.-S. Huang, Inorg. Chem. Commun. 4 (2001) 561.
[11] X.-M. Chen, B.-H. Ye, X.-C. Huang, Z.-T. Xu, J. Chem. Soc., Dalton Trans. (1996) 3465.
[12] W.D. Horrocks Jr., J.N. Ishley, R.R. Whittle, Inorg. Chem. 21 (1982) 3265.
[13] A.W. Addison, T.N. Rao, J. Reedijk, J. Van Rijn, G.C. Verschoor, J. Chem. Soc., Dalton Trans. (1984) 1349.
[14] J. Sanchiz, Y. Rodríguez-Martín, C. Ruiz-Pérez, A. Mederos, F. Lloret, M. Julve, New J. Chem. 26 (2002) 1624.
[15] A.L. Abuhijleh, C. Woods, Inorg. Chem. Commun. 4 (2001) 119.
[16] R. Carballo, A. Castiñeiras, B. Covelo, E.M. Vázquez-López, Polyhedron 20 (2001) 899.
[17] G.R. Desiraju, Acc. Chem. Res. 29 (1996) 441.
[18] C. Janiak, J. Chem. Soc., Dalton Trans. (2000) 3885.
[19] G.B. Deacon, R.J. Phillips, Coord. Chem. Rev. 33 (1980) 227.
[20] K. Nakamoto, Infrared and Raman Spectra of Inorganic and Coordination Compounds, 3rd ed., Wiley, New York, 1978.
[21] M. Melnik, Coord. Chem. Rev. 36 (1981) 287.
[22] E.A. Boudreaux, L.N. Mulay, Theory and Applications of Molecular Paramagnetism, Wiley, New York, 1976.
[23] S.K. Jain, B.S. Garg, Y.K. Bhoon, D.L. Klayman, J.P. Scovill, Spectrochim. Acta 41A (1985) 407.
[24] G.M. Sheldrick, SADABS, a program for absorption correction, University of Göttingen, Germany, 1996.
[25] G.M. Sheldrick, SHELXS-97, a program for the solution of crystal structures from X-ray data, University of Göttingen, Germany, 1997.
[26] G.M. Sheldrick, SHELXL-97, a program for the refinement of crystal structures from X-ray data, University of Göttingen, Germany, 1997.
[27] H.D. Flack, Helv. Chim. Acta 86 (2003) 905.
[28] E. Keller, SCHAKAL-97, a computer program for the graphic representation of molecular and crystallographic models, University of Freiburg, Germany, 1997.
[29] A.L. Spek, Acta Crystallogr. A46 (1990) C34, PLATON, Version 26-05-03.